Effects of incomplete decay in fluorescence lifetime estimation

Regina Won Kay Leung,[1,2,4] Shu-Chi Allison Yeh,[3,4] and Qiyin Fang[1,3,*]

[1]*Department of Engineering Physics, McMaster University, 1280 Main Street West, Hamilton, Ontario L8S 4K1, Canada*

[2]*Institute of Biomaterials & Biomedical Engineering, University of Toronto,164 College Street, Toronto, Ontario M5S 3G9, Canada*

[3]*School of Biomedical Engineering, McMaster University, 1280 Main Street West, Hamilton, Ontario L8S 4K1, Canada*

[4]*Contributed equally*

**qiyin.fang@mcmaster.ca*

Abstract: Fluorescence lifetime imaging has emerged as an important microscopy technique, where high repetition rate lasers are the primary light sources. As fluorescence lifetime becomes comparable to intervals between consecutive excitation pulses, incomplete fluorescence decay from previous pulses can superimpose onto the subsequent decay measurements. Using a mathematical model, the incomplete decay effect has been shown to lead to overestimation of the amplitude average lifetime except in mono-exponential decays. An inverse model is then developed to correct the error from this effect and the theoretical simulations are tested by experimental results.

OCIS codes: 180.2520 Fluorescence microscopy; (170.3650) Lifetime-based sensing

References and links

1. K. Suhling, P. M. French, and D. Phillips, "Time-resolved fluorescence microscopy," Photochem. Photobiol. Sci. **4**(1), 13–22 (2005).
2. M. T. Kelleher, G. Fruhwirth, G. Patel, E. Ofo, F. Festy, P. R. Barber, S. M. Ameer-Beg, B. Vojnovic, C. Gillett, A. Coolen, G. Kéri, P. A. Ellis, and T. Ng, "The potential of optical proteomic technologies to individualize prognosis and guide rational treatment for cancer patients," Target Oncol **4**(3), 235–252 (2009).
3. I. Munro, J. McGinty, N. Galletly, J. Requejo-Isidro, P. M. P. Lanigan, D. S. Elson, C. Dunsby, M. A. A. Neil, M. J. Lever, G. W. H. Stamp, and P. M. W. French, "Toward the clinical application of time-domain fluorescence lifetime imaging," J. Biomed. Opt. **10**(5), 051403 (2005).
4. J. R. Lakowicz, *Principles of Fluorescence Spectroscopy*, 3rd ed. (Kluwer Academic/Plenum, New York, 2006), Chap. 4.
5. G. O. Fruhwirth, S. Ameer-Beg, R. Cook, T. Watson, T. Ng, and F. Festy, "Fluorescence lifetime endoscopy using TCSPC for the measurement of FRET in live cells," Opt. Express **18**(11), 11148–11158 (2010).
6. T. Ng, A. Squire, G. Hansra, F. Bornancin, C. Prevostel, A. Hanby, W. Harris, D. Barnes, S. Schmidt, H. Mellor, P. I. H. Bastiaens, and P. J. Parker, "Imaging protein kinase Calpha activation in cells," Science **283**(5410), 2085–2089 (1999).
7. E. A. Jares-Erijman and T. M. Jovin, "Imaging molecular interactions in living cells by FRET microscopy," Curr. Opin. Chem. Biol. **10**(5), 409–416 (2006).
8. Y. Chen and A. Periasamy, "Characterization of two-photon excitation fluorescence lifetime imaging microscopy for protein localization," Microsc. Res. Tech. **63**(1), 72–80 (2004).
9. J. R. Lakowicz, H. Szmacinski, K. Nowaczyk, W. J. Lederer, M. S. Kirby, and M. L. Johnson, "Fluorescence lifetime imaging of intracellular calcium in COS cells using Quin-2," Cell Calcium **15**(1), 7–27 (1994).
10. A. V. Agronskaia, L. Tertoolen, and H. C. Gerritsen, "Fast fluorescence lifetime imaging of calcium in living cells," J. Biomed. Opt. **9**(6), 1230–1237 (2004).
11. G. Wagnières, J. Mizeret, A. Studzinski, and H. van den Bergh, "Frequency-domain fluorescence lifetime imaging for endoscopic clinical cancer photodetection: apparatus design and preliminary results," J. Fluoresc. **7**(1), 75–83 (1997).
12. Y. Sun, N. Hatami, M. Yee, J. Phipps, D. S. Elson, F. Gorin, R. J. Schrot, and L. Marcu, "Fluorescence lifetime imaging microscopy for brain tumor image-guided surgery," J. Biomed. Opt. **15**(5), 056022 (2010).
13. J. A. Russell, K. R. Diamond, T. Collins, H. F. Tiedje, J. E. Hayward, T. J. Farrell, M. S. Patterson, and Q. Fang, "Characterization of fluorescence lifetime of photofrin and delta-aminolevulinic acid induced protoporphyrin IX

#146904 - $15.00 USD Received 2 May 2011; revised 21 Jul 2011; accepted 31 Jul 2011; published 2 Aug 2011

in living cells using single and two-photon excitation," IEEE J. Sel. Top. Quantum Electron. **14**(1), 158–166 (2008).
14. A. Rück, Ch. Hülshoff, I. Kinzler, W. Becker, and R. Steiner, "SLIM: a new method for molecular imaging," Microsc. Res. Tech. **70**(5), 485–492 (2007).
15. W. Becker, A. Bergmann, and C. Biskup, "Multispectral fluorescence lifetime imaging by TCSPC," Microsc. Res. Tech. **70**(5), 403–409 (2007).
16. H. C. Gerritsen, "High-speed fluorescence lifetime imaging," Proc. SPIE **5323**, 77–87 (2004).
17. W. Becker, *The bh TCSPC Handbook*, 3rd ed. (Becker & Hickl GmbH, 2008)
18. P. R. Barber, S. M. Ameer-Beg, J. Gilbey, L. M. Carlin, M. Keppler, T. C. Ng, and B. Vojnovic, "Multiphoton time-domain fluorescence lifetime imaging microscopy: practical application to protein-protein interactions using global analysis," J. R. Soc. Interface **6**(0), S93–S105 (2009).
19. P. R. Barber, S. M. Ameer-Beg, J. Gilbey, R. J. Edens, I. Ezike, and B. Vojnovic, "Global and pixel kinetic data analysis for FRET detection by multi-photon time-domain FLIM," Proc. SPIE **5700**, 171–181 (2005).
20. J. Stewart, *Calculus: Early Transcendentals*, 5th ed. (Thomson/Brooks/Cole, Belmont, CA, 2003)
21. J. R. Taylor, *An Introduction to Error Analysis*, 2nd ed. (University Science Books, Sausalito, 1997)
22. D. J. Schroeder, *Astronomical Optics* (Academic Press, San Diego, 2000), Chap. 17.
23. Y. Yuan, T. Papaioannou, and Q. Fang, "Single-shot acquisition of time-resolved fluorescence spectra using a multiple delay optical fiber bundle," Opt. Lett. **33**(8), 791–793 (2008).

1. Introduction

Fluorescence lifetime imaging microscopy (FLIM) has become a powerful imaging tool in cell and molecular biology research [1], drug discovery [2], and clinical diagnosis [3]. Fluorescence lifetime can be defined as the average time fluorophores stay in the excited state after excitation and described by multiple exponential decays [4]. Given sufficient signal, fluorescence lifetime is independent of fluorescent intensity such that it has been used to complement steady state imaging modalities, which are based on intensity and spectral features [4]. FLIM based techniques have been extensively investigated in a number of applications including Fluorescent Resonant Energy Transfer (FRET) [5–8], ion mapping of intracellular environment [9,10], as well as clinical diagnosis for malignant tumours [11,12] and dosimetry for drug administration [13,14].

In time-domain measurement, a short-pulsed laser is used to excite the fluorophores and the fluorescent emission is measured as a function of intensity decay over time [4]. The fluorescence decay may be modeled as the summation of multiple exponential components, as shown in Eq. (1).

$$F(t) = a_1 e^{-t/\tau_1} + a_2 e^{-t/\tau_2} + a_3 e^{-t/\tau_3} + \cdots \quad (1)$$

Here $F(t)$ is the measured fluorescence intensity as a function of time t; τ_i are the individual exponential components; and a_i are the coefficients of each exponential term. The measured intensity decay is a convolution of $F(t)$ with the Instrument Response Function (IRF); thus deconvolution is sometimes necessary to recover the $F(t)$ when the IRF is not negligible [4].

Typical FLIM systems use either Time Correlated Single Photon Counting (TCSPC) based point scanning method [6,13–15] or ICCD-based wide-field imaging technique [3,9,11,16]. In TCSPC, only the first photon of a pulse is recorded. To build a probability histogram for each pixel in an image, a large number of pulses are needed. In ICCD based techniques, each pulse excites the whole field-of-view while a large number of excitation pulses are also needed to achieve sufficient signal-to-noise ratio (SNR). Consequently, both techniques require high repetition rate light source and detection systems in order to accurately determine the fluorescence lifetime while achieving sufficient imaging frame rate. Since short, sub-nanosecond pulsed excitation is also required in time-domain systems, mode-locked Ti:sapphire lasers have become the most commonly used excitation sources in current FLIM systems. New picosecond diode lasers with various excitation wavelengths also holds promise for several biological applications.

In Ti:sapphire lasers, the repetition rate is typically limited to 70–100 MHz due to the mode-locking mechanism. This limitation has caused concerns in measuring longer decays where the average fluorescence lifetime is comparable to the period of the excitation pulses

#146904 - $15.00 USD Received 2 May 2011; revised 21 Jul 2011; accepted 31 Jul 2011; published 2 Aug 2011

[4,16]. It has been advised that the interval between two excitation pulses should be more than four [4] or five [16] times of the average fluorescence lifetime in order to accurately estimate the lifetime from experiments. That is, if a fluorophore's lifetime is longer than 3 ns and a 80 MHz (12.5 ns between excitation pulses) laser is used, the tails of decay curves from previous excitation periods may contribute significantly to the current decay curve, which may lead to inaccurate lifetime estimation [16,17]. This "incomplete decay" effect is illustrated in Fig. 1. To simplify the illustration, the commonly seen noise background or instrument offset is ignored here.

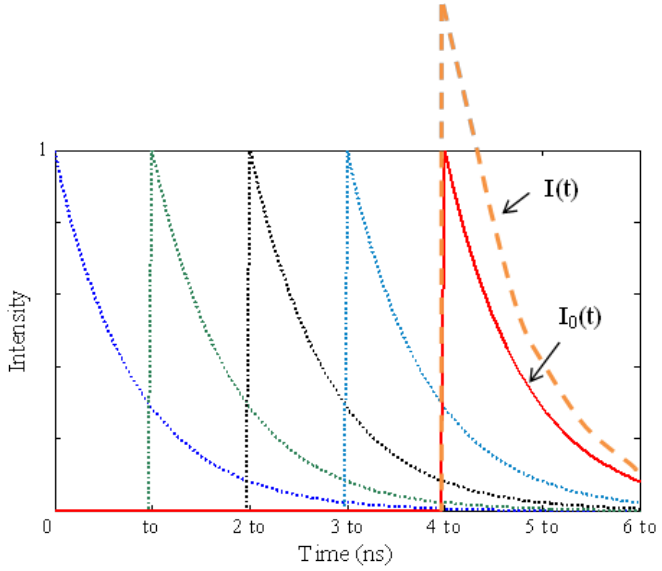

Fig. 1. Simulated effect of incomplete decay on the measured decay curve is illustrated, where the tails of multiple previous decay curves (short dashed lines) excited by a high repetition rate light source contribute significantly to the current original curve, $I_0(t)$(solid line), which lead to the distorted measured decay curve, I(t) (long dashed line) that can cause inaccurate lifetime estimation. t_0 is the time interval between two consecutive excitation pulses. Note that the incomplete decay caused by the laser excitation prior to the current one contributes the most to the current measured decay curve as illustrated in the last decay curve.

In practice, many fluorophores have long lifetimes that are subjected to the influence of the incomplete decay effect when excited by high repetition rate lasers. For example, a clinically-approved photosensitizer for photodynamic therapy (PDT), Photofrin®, is a typical long-lived fluorophore with its average lifetime of around 13 ns in bulk solutions or 6 –10 ns in live cells [13,14]. Incomplete decay may also cause problems in applications using short lifetime fluorophores. An example is FLIM based Föster Resonant Energy Transfer or FLIM-FRET, where protein-protein interactions is calculated from small changes of donor fluorophore lifetimes [7]. Many FRET pairs exhibit bi-exponential decays with fluorescence lifetimes of 2–4 ns [8], while the lifetime change in the order of 0.1–0.2 ns is critical.

The inaccurate lifetime estimation due to the ultrafast repetitive excitation is generally mentioned [4,18] and Barber *et al.,* initially reported an analytical model in a conference paper [19] to describe the "incomplete decay" effect. This original work is crucial towards designing time-domain instrumentations and selection of light sources. In practical situations, however, excitation repetition rate is not a typical selectable feature. In addition, a large number of data has already been acquired using high repetition rate excitation sources. In this report, we established an analytical model similar to that of Barber *et al.* to simulate the effects of the incomplete decay and quantitatively determine the influence of the incomplete decay to the accuracy of lifetime parameter estimation either in noise-free or noisy conditions.

#146904 - $15.00 USD Received 2 May 2011; revised 21 Jul 2011; accepted 31 Jul 2011; published 2 Aug 2011

The theoretical simulation is experimentally tested using standard fluorophores with a multiphoton microscope and a 80 MHz Ti:sapphire laser. Most importantly, correction methods were developed to recover original lifetime parameters from the measured lifetime values. Table 1 illustrated the abbreviations used in the rest of this article.

Table 1. Definition of the abbreviations for lifetimes

Abbreviations	*Definition*
τ_0	Original amplitude weighted lifetime
τ_{id}	Simulated measured amplitude weighted lifetime due to incomplete decay alone
τ_{idn}	Simulated measured amplitude weighted lifetime due to incomplete decay and with noise

2. Methods

2.1. Analytical model of incomplete decay

The analytical model describing the incomplete decay effect is first reported by Barber *et al.* in Ref. [19]. As shown in Fig. (1), the original fluorescence intensity decay $I_0(t)$ is different from the measured decay curve $I(t)$, where the period of the excitation laser pulses are short compared to the fluorophore's lifetime. If $I_0(t)$ is represented with N exponential terms, it can be described as:

$$I_0(t) = A_{01}e^{-t/\tau_{01}} + A_{02}e^{-t/\tau_{02}} + \ldots + A_{0i}e^{-t/\tau_{0i}} + \ldots + A_{0N}e^{-t/\tau_{0N}} \quad (2)$$

where for the i^{th} term, τ_{0i} is the lifetime component. Then, the original amplitude weighted lifetime τ_0 is determined by [4]

$$\tau_0 = A^n{}_{01}\tau_{01} + A^n{}_{02}\tau_{02} + \ldots + A^n{}_{0N}\tau_{0N} \quad (3)$$

where A^n_{0i} is the normalized coefficient defined as $A^n_{0i} = A^n_{0i} \Big/ \sum_{i=1}^{N} A^n_{0i}$.

Similarly, the experimentally measured fluorescence decay $I(t)$ and estimated lifetime τ are [4]

$$I(t) = A^n{}_1 e^{-t/\tau_1} + A^n{}_2 e^{-t/\tau_2} + \ldots + A^n{}_N e^{-t/\tau_N} \quad (4)$$

$$\tau = A^n{}_1\tau_1 + A^n{}_2\tau_2 + \ldots + A^n{}_N\tau_N \quad (5)$$

where $A^n{}_i$ is the normalized coefficient defined as $A^n_i = A^n_i \Big/ \sum_{i=1}^{N} A^n_i$.

Both the measured and original multi-exponential decay curves are characterized by their corresponding coefficients and lifetime components. To demonstrate how incomplete decay influences fluorescence lifetime measurement and estimation, a forward model was developed while assuming the original parameters (A_{01}, $A_{02,}$…, A_{0N}, τ_{01},τ_{02},…,τ_{0N}) are known and that the measured parameters affected by incomplete decay (A_1, $A_{2,}$…, A_N, τ_1,τ_2,…,τ_N) are unknown. In practice, one would always obtain the measured values experimentally and try to estimate the original set of decay parameters. An inverse model was then derived from the forward model and assumes the opposite: the measured parameters are known and the original parameters are unknown. The goal of the inverse model is to predict the original lifetime parameters from the measured data by correcting errors in lifetime estimation due to incomplete decay.

Please note that in the following analysis, we made an assumption that there are an unlimited number of fluorophores available in the system, while only a small number of them are excited at any given time. In practice, this assumption is probably valid especially for multiphoton FLIM measurements while only the focal plane is excited by high repetition rate (70-100 MHz) mode-locked Ti: Sapphire lasers. In these cases, photobleaching is also not

#146904 - $15.00 USD Received 2 May 2011; revised 21 Jul 2011; accepted 31 Jul 2011; published 2 Aug 2011

significant. One should note that especially in TCSPC measurements where a large number of excitation pulses are used, this assumption may be invalid.

2.1.1. Forward Model

From Fig. 1, as a result of incomplete decay, $I(t)$ is a summation of $I_0(t)$ and the tails of the n previous decay curves where $I_0(t)$ is the original decay curve, $I(t)$ is the resulting measured decay curve, and t_o is the time interval between two consecutive excitation pulses:

$$I(t) = \lim_{n\to\infty}[I_0(t) + I_0(t+t_o) + \ldots + I_0(t+nt_o)] \tag{6}$$

Substituting in Eq. (2) into Eq. (6) yields

$$I(t) = \lim_{n\to\infty}\left(\sum_{i=1}^{N} A_{0i}e^{-\frac{t}{\tau_{0i}}} + \sum_{i=1}^{N} A_{0i}e^{-\frac{t+t_0}{\tau_{0i}}} + \ldots + \sum_{i=1}^{N} A_{0i}e^{-\frac{t+nt_0}{\tau_{0i}}}\right) = \sum_{i=1}^{N}\left(A_{0i}e^{-\frac{t}{\tau_{0i}}}\cdot\sum_{n=0}^{\infty}e^{-\frac{nt_0}{\tau_{0i}}}\right) \tag{7}$$

Since $\sum_{n=0}^{\infty} r^n = 1/(1-r)$ for $|r|<1$, while $|e^{-t_0/\tau_{0i}}|<1$ as t_o and τ_{0i} are always positive, the final expression for $I(t)$ can be significantly simplified to [20]

$$I(t) = \sum_{i=1}^{N}\frac{A_{0i}}{1-e^{-t_0/\tau_{0i}}}e^{-t/\tau_{0i}} \tag{8}$$

Therefore, by comparing Eq. (8) with Eq. (4), the measured parameters can now be expressed as a function of the original parameters where

$$A_i = \frac{A_{0i}}{1-e^{-t_0/\tau_{0i}}} \tag{9}$$

$$\tau_i = \tau_{0i} \tag{10}$$

The measured amplitude weighted lifetime due to the effect of incomplete decay (τ_{id}) can be calculated from original parameters by substituting Eqs. (9) and (10) into Eq. (5):

$$\tau_{id} = \sum_{i=1}^{N}\frac{A_{0i}/(1-e^{-t_0/\tau_{0i}})}{\sum_{k=1}^{N}A_{0k}/(1-e^{-t_0/\tau_{0k}})}\tau_{0i} \tag{11}$$

Finally, to quantify the difference between measured and original amplitude weighted lifetimes, the fractional error is defined as

$$\%E = \frac{\tau_{id} - \tau_0}{\tau_0}\times 100\% \tag{12}$$

2.1.2. Inverse Model

The inverse model is derived from the forward model by rearranging Eqs. (9) and (10) to describe original parameters in terms of measured parameters as shown in Eqs. (13) and (14).

$$A_{0i} = A_i(1-e^{-\frac{t_o}{\tau_i}}) \tag{13}$$

$$\tau_{0i} = \tau_i \tag{14}$$

As shown in Eq. (15), the original amplitude weighted lifetime can be expressed in terms of the measured parameters by substituting Eqs. (13) and (14) into Eq. (3) as indicated by

$$\tau_0 = \sum_{i=1}^{N}\frac{A_i(1-e^{-t_0/\tau_i})}{\sum_{k=1}^{N}A_k(1-e^{-t_0/\tau_i})}\tau_i \tag{15}$$

#146904 - $15.00 USD Received 2 May 2011; revised 21 Jul 2011; accepted 31 Jul 2011; published 2 Aug 2011

Finally, to quantify the difference between original and measured amplitude weighted lifetimes, the fractional error is defined as

$$\%E = \frac{\tau_0 - \tau_{id}}{\tau_{id}} \times 100\% \tag{16}$$

The inverse analytical model can be applied directly to the measured parameters to correct for the effects of incomplete decay and obtain the original amplitude weighted lifetime value. The analytical model is also further examined to create guidelines for lifetime measurements to determine whether or not incomplete decay is significant to require correction.

From the results given by Eq. (8), Eq. (15), and Eq. (16) in the mono-exponential decay case, incomplete decay does not affect the estimated amplitude weighted lifetimes (τ_{id}) since the τ_{id} is the same as the original individual lifetime while the coefficient is normalized.

As most of the commonly used fluorophores exhibit multiple-exponential decay, this study focuses on how the incomplete decay contributes to incorrect lifetime estimation in the bi-exponential cases, which is mostly seen in practical FLIM experiments. Nonetheless, the inverse model can be applied to more complex cases where more than two exponential components are present. The general analytical model for multi-exponential incomplete decay developed above can be applied to the specific bi-exponential case as shown below where N = 2. Expressing the measured coefficients and component lifetimes affected by incomplete decay in terms of the original parameters using Eq. (9) and (10),

$$A_1 = \frac{A_{01}}{1 - e^{-\frac{t_o}{\tau_{01}}}} \tag{17}$$

$$A_2 = \frac{A_{02}}{1 - e^{-\frac{t_o}{\tau_{02}}}} \tag{18}$$

$$\tau_1 = \tau_{01} \tag{19}$$

$$\tau_2 = \tau_{02} \tag{20}$$

The measured amplitude weighted lifetime is given by

$$\tau_{id} = A^n{}_1 \tau_1 + A^n{}_2 \tau_2 \tag{21}$$

$$\tau_{id} = \frac{\frac{A_{01}}{1 - e^{-t_o/\tau_{01}}}}{\frac{A_{01}}{1 - e^{-t_o/\tau_{01}}} + \frac{A_{02}}{1 - e^{-t_o/\tau_{02}}}} \tau_1 + \frac{\frac{A_{02}}{1 - e^{-t_o/\tau_{02}}}}{\frac{A_{01}}{1 - e^{-t_o/\tau_{01}}} + \frac{A_{02}}{1 - e^{-t_o/\tau_{02}}}} \tau_2 \tag{21a}$$

where the measured amplitude weighted lifetime (τ_{id}) as shown in Eq. (21a) is expressed in terms of the original parameters by substituting Eq. (17) to Eq. (20) into Eq. (21). Again, applying the general analytical model developed above, the inverse model is applied to the bi-exponential case where N = 2 to obtain the following equations to express the original parameters in terms of measured parameters:

$$A_{01} = A_1 (1 - e^{-\frac{t_o}{\tau_1}}) \tag{22}$$

$$A_{02} = A_2 (1 - e^{-\frac{t_o}{\tau_2}}) \tag{23}$$

$$\tau_{01} = \tau_1 \tag{24}$$

#146904 - $15.00 USD Received 2 May 2011; revised 21 Jul 2011; accepted 31 Jul 2011; published 2 Aug 2011

$$\tau_{02} = \tau_2 \tag{25}$$

The original amplitude weighted lifetime is

$$\tau_0 = A_{01}\tau_{01} + A_{02}\tau_{02} \tag{26}$$

$$\tau_0 = \frac{A_1(1-e^{-t_o/\tau_1})}{A_1(1-e^{-t_o/\tau_1}) + A_2(1-e^{-t_o/\tau_2})}\tau_{01} + \frac{A_2(1-e^{-t_o/\tau_2})}{A_1(1-e^{-t_o/\tau_1}) + A_2(1-e^{-t_o/\tau_2})}\tau_{02} \tag{26a}$$

where the original amplitude weighted lifetime as shown in Eq. (26a) is expressed in terms of the measured parameters by substituting Eqs. (22) to (25) into Eq. (26).

2.1.3. Incomplete Decay Simulations

To further investigate the analytical models and develop guidelines to determine the significance of incomplete decay on amplitude weighted lifetime measurements, bi-exponential incomplete decay curves of different lifetimes are simulated in Matlab under various conditions. Conditions include varying the repetition rate, coefficients, and differences in lifetime components. The fractional error between the original (τ_0) and simulated measured amplitude weighted lifetime (τ_{id}) as defined in Eq. (12) or (16) is calculated using the derived analytical models and examined under each condition.

2.2. Noise simulation

To understand the effect of the incomplete decay in practical experiments, noise simulation has been performed to see whether lifetime estimation error caused by random experimental noise is comparable to errors from incomplete decay. Typical experimental noise sources in FLIM measurements include shot noise (Poisson noise) from the photo detector, digitization error from the digitizer, ambient light, and other electronics noise from the amplification process. In general, the signal amplitude is low and instrumentation noises significantly surpassed the shot noise. In this work, we assume the errors arise from these processes are independent of each other. Consequently, although each process may have a different error distribution, the overall error can be considered to be Gaussian [21]. Therefore, in the noise simulation, Gaussian noise is generated and added to the simulated mono- and bi-exponential incomplete decay curves at different SNR values. Specifically, the SNR is defined as the average signal amplitude divided by random Gaussian noise with standard deviation "sd" [22]. Curve fitting was then performed on the noisy simulated curves to determine the lifetime parameters and the fractional errors.

To simulate mono- and bi-exponential incomplete decay curves, all the parameters were defined according to the experimental conditions. For mono-exponential, two cases were simulated: Case 1 with τ_1 = 1.5 ns and Case 2 with τ_2 = 4.9 ns which correspond to the lifetimes of Rhodamine B (RdmB) and Lucifer Yellow (LY) respectively. For bi-exponential, various cases were generated with different A_1:A_2 ratios where A_1 ranged from 0.1 – 0.9 and A_2 is normalized to be 1 – A_1. In all the cases, the original coefficient values were chosen such that $A_1 + A_2 = 516$, τ_1 = 1.5 ns (RdmB), and τ_2 = 4.9 ns (LY). The absolute original coefficient values were set as 516 based on typical original peak decay intensities obtained from the real TCSPC experiments; however, it will not affect the actual calculation of amplitude weighted lifetime, where the normalized coefficients were used. Although the fitting coefficient A in mono-exponential decay is not critical, we performed and plotted simulation to demonstrate the effect of noise on parameter estimations.

Gaussian noise was then generated with a mean of 0 and a standard deviation (SD) based on the signal to noise ratio (SNR) where SNR was defined as the average signal amplitude divided by SD of random Gaussian noise. The range of SNR in our simulations ranged from 16 to 182 and was determined by our typical experimental data measured using a 2-photon

#146904 - $15.00 USD Received 2 May 2011; revised 21 Jul 2011; accepted 31 Jul 2011; published 2 Aug 2011

microscope and a TCSPC FLIM module. The generated Gaussian noise at various SNR is then added to the simulated incomplete decay curves.

Curve fitting to the simulated data was then performed using the curve fitting toolbox (Matlab v2010, Mathworks, Natick, MA), where the non-linear least squares method using the Trust-Region algorithm was applied. Fitted parameters (A_1, A_2, τ_1, τ_2) were used to calculate lifetime values and the fractional error for various SNR. The fractional error between the data with and without the noise is defined as $(\tau_{idn}-\tau_0)/\tau_0 * 100$, where τ_{idn} represents the amplitude weighted average lifetime of the noisy incomplete decay curve and τ_0 represents the amplitude weighted average lifetime of the original decay curve.

2.3. Time-domain multi-photon fluorescence lifetime measurements

To validate the theoretical model and simulations, we measured the fluorescence lifetime of standard fluorophores using two fluorescence lifetime measurement modalities: a time-domain FLIM microscope using 80 MHz laser excitation and a second set of measurements using a frequency domain lifetime fluorometer.

The time-domain FLIM instrument is a two-photon microscope (TSC SP5 & DMI 6000 B, Leica, Wetzlar, Germany) equipped with the TCSPC fluorescence lifetime acquisition module (SPC-830, Becker & Hickle GmbH, Berlin, Germany) and a femtosecond mode-locked Ti:sapphire laser pulsing at 80 MHz (Chameleon-Ultra, Coherent. Santa Clara, CA). In this system, fluorescence emission channels are selected by a prism and several variable-width slits in front of detectors. The fluorescence intensity decay was fitted to a bi-exponential decay model using the Matlab curve fitting toolbox to calculate the lifetime parameters.

The frequency domain instrument is a lifetime fluorometer (ChronosFD, ISS, Champaign, IL) using a laser diode centred at 470 nm (90099, ISS) with the modulation frequency between 8 to 200 MHz. The fluorescence was transmitted through a band pass filter centred at 580 nm (580/DF30, XF3022, Omega Optical, VT), and the detected signal was analyzed using the included software (Vinci, ISS) to retrieve the time-domain parameters.

Two standard fluorescence dyes, Lucifer yellow (LY) (L0259, Sigma-Aldrich, St. Louis, MO) with a lifetime of 4.9 ns and Rhodamine B (RdmB) (R6626, Sigma-Aldrich) with a lifetime of 1.5 ns were diluted in purified water to the concentration of 2 μM. The two fluorescence dyes were then mixed at appropriate ratios and their lifetimes are measured using both instruments for comparison. In the frequency-domain measurements, Coumarin 6 (546283, Sigma-Aldrich) was used as a reference dye with the fluorescence lifetime of 2.5 ns and excitation and emission spectra overlapping with LY and RdmB. It was diluted in 99.9% Ethanol (34964, Sigma Aldrich) to appropriate concentration that provides comparable signals with respect to the samples. To provide references for the original amplitude weighted lifetime calculation, the fluorescence lifetimes of LY and RdmB were then retrieved by mono-exponential fitting using Vinci (data not shown). In the time-domain measurements, the samples were illuminated with the laser at 860 nm and the emission channel was set from 500 nm to 700 nm to ensure the optimum excitation and detection efficiency. Three separate measurements have been performed and all the acquisition parameters remained the same throughout the acquisition processes to eliminate artefacts from sources other than the incomplete decay. Quantum efficiency correction was also performed after the data acquisition by comparing the integrated photon intensities of each fluorescence dye; therefore the real contribution of individual lifetimes can be restored.

3. Results

3.1. Simulated results of the incomplete decay

According to Eq. (8), incomplete decay only affects the coefficient values, while the measured individual lifetime components are the same as the original individual lifetime components, as indicated in Eqs. (9) and (10). Therefore, amplitude weighted lifetime estimation for mono-

#146904 - $15.00 USD Received 2 May 2011; revised 21 Jul 2011; accepted 31 Jul 2011; published 2 Aug 2011

exponential decay is unaffected by incomplete decay because its amplitude weighted lifetime estimation does not depend on the coefficient. For bi-exponential decays, however, the measured amplitude weighted lifetime (τ_{id}) does depend on the coefficients A_1 and A_2, where $\tau_{id} = A_1\tau_1 + A_2\tau_2$. Thus, measured parameters from bi-exponential decay must be interpreted carefully and corrected for incomplete decay. The rest of the report will focus on examining the analytical model for incomplete decay for bi-exponential cases. The illustration of the effect of incomplete decay on mono- and bi-exponential decay is shown in Fig. 2 where both the original (τ_0) and measured (τ_{id}) decay curves are shown on a linear and log scale. As shown in Fig. 2, incomplete decay only affects the estimation of amplitude weighted lifetimes for bi-exponential decays. Table 2 shows the time-domain parameters distorted by the incomplete decay in mono- and bi-exponential cases used in Fig. 2.

The difference between the i^{th} measured and original coefficients which is defined as the fractional error $E_i = (A_i - A_{0i})/A_{oi,}$ where i = 1, 2 for bi-exponential cases. According to Eq. (9), E_i can be rewritten as

$$E_i = \frac{1}{1-e^{-t_0/\tau_i}} - 1 \tag{27}$$

As a result of the dependence of amplitude weighted lifetimes on the individual coefficients given by Eq. (20), parameters that result in less than 5% fractional errors between the individual measured and original coefficients which would then result in less than %5 uncertainty in lifetime estimations are investigated. Given the typical temporal resolution of about 200 ps in time-domain instruments, we consider 5% uncertainty in lifetime estimation can be considered as acceptable error. As a result, when the fractional error caused by incomplete decay is less than 5%, it is considered insignificant and can be neglected. One should note that this 5% cutoff value is somewhat arbitrary and, depending on the application, it should be used with caution. Consequently, since the magnitude of the ith fractional error (E_i) is only dependent on the ith individual lifetime (τ_i), the threshold value of individual

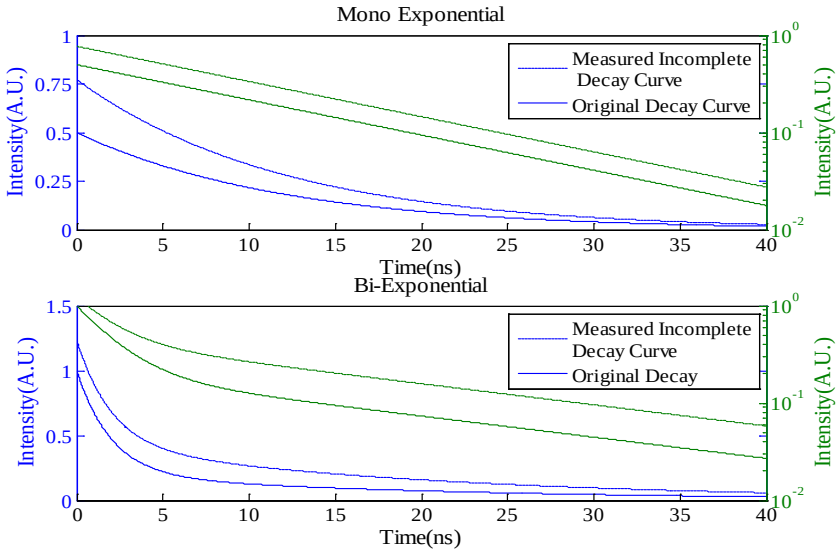

Fig. 2. Simulation of the original (solid line) and measured (dashed line) decay curves for both mono-exponential (top) and bi-exponential (bottom) cases at repetition rate of 80 MHz (12.5 ns). For the mono-exponential case, τ_{01} = 12 ns, A_{01} = 0.5. For the bi-exponential case, τ_{01} = 2 ns, τ_{02} = 20 ns, A_{01} = 0.8, A_{02} = 0.2. The corresponding log scale plots of each decay curve are also shown as the top two curves of each graph with the log plot axis on the right.

#146904 - $15.00 USD Received 2 May 2011; revised 21 Jul 2011; accepted 31 Jul 2011; published 2 Aug 2011

lifetimes($\tau_{i(thld)}$) that would give fractional errors of 5% is determined by rearranging Eq. (26). The threshold value is expressed as:

$$\tau_{i(thld)} = -\frac{t_o}{\ln(0.05/1.05)} \tag{28}$$

Also, as shown in Eq. (27), E_i is a monotonically increasing function with respect to τ_i, which means if $\tau_i < \tau_{i(thld)}$, the estimation errors due to incomplete decay are less than 5% and may be negligible. The $\tau_{i(thresh)}$ values corresponding to various laser repetition rates are shown in Table 3. As expected, the higher the repetition rate, the lower the threshold individual lifetime value, and thus the more likely incomplete decay will cause fractional errors between coefficients and cause errors in lifetime parameter estimation.

It is also useful to note that the fractional error E_i scales linearly with the laser repetition period t_o and thus the individual threshold lifetime values ($\tau_{i(thld)}$) that would give fractional errors of 5% can instead be expressed as a fraction of the repetition period, $t_o/\tau_{i(thld)}$. This threshold ratio between repetition period t_o and threshold lifetime value $\tau_{i(thld)}$ can be denoted as $R_{i(thld)}$. By re-arranging Eq. (28), $R_{i(thld)} = t_o/\tau_{i(thld)} = -\ln(0.05/1.05) = 3.045$. Since E_i is a monotonically decreasing function with respect to t_o/τ_i, this means that as long as the time interval between laser pulses (t_o) is 3 times longer than the individual lifetime τ_i, the estimation errors due to incomplete decay are less than 5% and may be negligible.

When the individual lifetimes are longer than those specified in Table 3 for corresponding repetition rates, the superposition from previous decay can affect lifetime parameter estimation significantly. To develop guidelines that determine the significance of incomplete decay in lifetime measurements, it is of great interest to investigate incomplete decay in various experimental conditions (e.g. repetition rate, coefficients, difference in lifetime components).

Table 2. Original and measured parameters for mono- and bi-exponential decay

Mono-exponential		Bi-exponential	
Original	Measured (τ_{id})	Original	Measured (τ_{id})
$A_{01} = 0.50$	$A_1 = 0.77$	$A_{01} = 0.80$	$A_1 = 0.80$
$\tau_{01} = 12$ ns	$\tau_1 = 12$ ns	$A_{02} = 0.20$	$A_2 = 0.43$
$\tau_0 = 12$ ns	$\tau_{id} = 12$ ns	$\tau_{01} = 2.0$ ns	$\tau_1 = 2.0$ ns
		$\tau_{02} = 20$ ns	$\tau_2 = 20$ ns
		$\tau_0 = 5.6$ ns	$\tau_{id} = 8.29$ ns

Table 3. Threshold amplitude averaged lifetime values (for bi-exponential decay) at various time windows (t_o) between consecutive excitation pulses

t_o (ns)	$\tau_{i(thresh)}$ (ns)
10 (100 MHz)	3.28
12.5 (80 MHz)	4.11
16.7 (60 MHz)	5.49
25 (40 MHz)	8.21
50 (20 MHz)	16.4

As shown in Fig. 3, the fractional error between original and measured amplitude weighted lifetimes as defined in Eq. (12) corresponding to a set of original parameters ($A_{01} = A_{02} = 0.5$, $\tau_{01} = 1$ ns, τ_{02} varies from 0 to 20 ns) was plotted with respect to τ_2 at various repetition rates as shown by the multiple curves. It was observed that at each τ_2 value, the error increased as the repetition rate increased. For example, the error of the τ_{id} at τ_2 of 20 ns at the highest repetition rate (100 MHz) resulted in the maximum error of all cases with 40% error from the original average lifetime value (τ_0). Figure 3 also illustrated the negligible incomplete decay effect when $\tau_1 = 1$ ns and $\tau_2 < \tau_{i(thld)}$; the error is always less than 5%. Similarly, Fig. 3 illustrates that when the time window between laser excitation pulses (t_o) is around three times longer than both τ_1 and τ_2, the error due to incomplete decay is less than 5%.

#146904 - $15.00 USD Received 2 May 2011; revised 21 Jul 2011; accepted 31 Jul 2011; published 2 Aug 2011

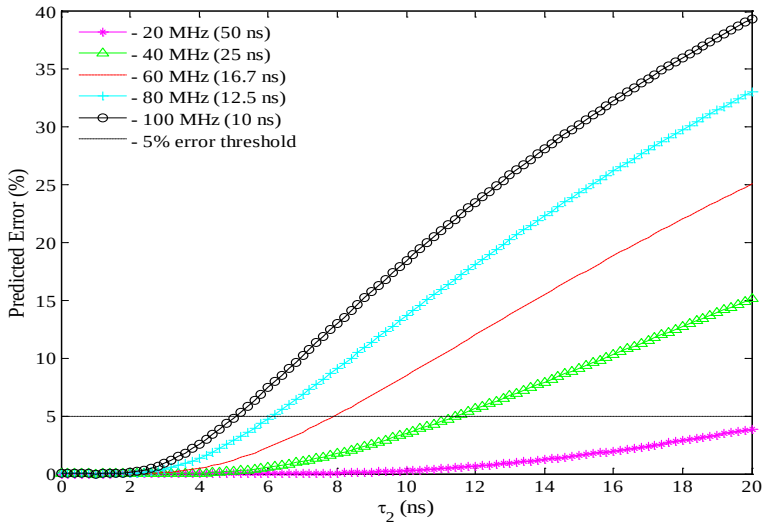

Fig. 3. The predicted fractional errors defined by Eq. (12) are plotted as a result of incomplete decay at various original amplitude weighted lifetime values at various repetition rates for bi-exponential decays. For each curve, τ_1 remains constant at 1 ns and τ_2 is varied from 0 to 20 ns as shown on the x-axis. The coefficients are fixed at $A_{o1} = A_{o2} = 0.5$.

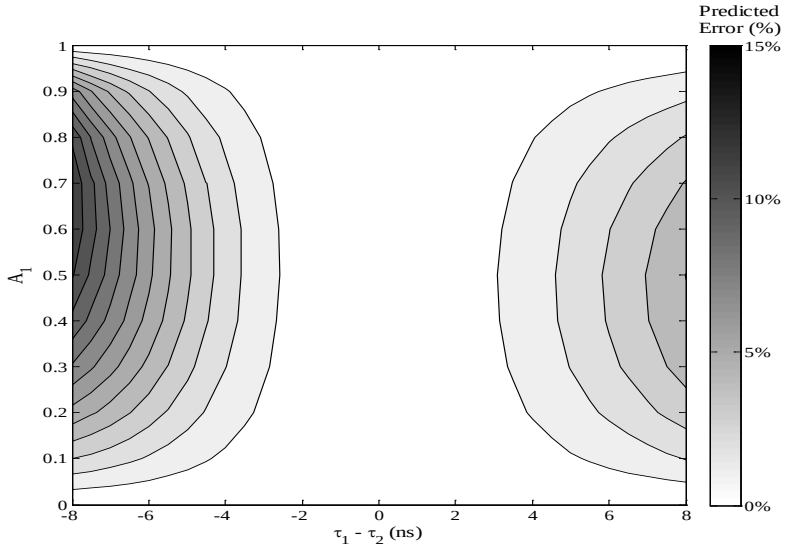

Fig. 4. – Illustrating the dependence and trends of absolute fractional error (as defined in Eq. (16) on measured coefficient and lifetime component values using a contour plot. Y-axis corresponds to A_1 and is varied from 0 to 1 ($A_2 = 1 - A_1$). X-axis corresponds to the difference between measured lifetime components ($\tau_1 - \tau_2$) where τ_2 (10 ns) was chosen to be constant and τ_1 varies from $\tau_2 - 8$ (2 ns) to $\tau_2 + 8$ (18 ns). The varying gray scale color of the contour map corresponds to the calculated absolute fractional errors where the larger the error, the darker the gray scale color as defined by the color bar.

The effect of measured coefficients and lifetime component values on the absolute fractional error between τ_{id} and τ_0 values as defined in Eq. (16) was also investigated at a constant repetition rate of 80 MHz as shown in Fig. 4. Figure 4 shows a contour plot where to the difference between measured lifetime components ($\tau_1 - \tau_2$) where τ_2 (10 ns) was chosen to

#146904 - $15.00 USD Received 2 May 2011; revised 21 Jul 2011; accepted 31 Jul 2011; published 2 Aug 2011

be constant and τ_1 varies from $\tau_2 - 8$ (2 ns) to $\tau_2 + 8$ (18 ns). The varying gray scale color of the contour map corresponds to the calculated absolute fractional errors for the various corresponding measured coefficient and lifetime component values where the darker the color, the larger the error.

Examining the effect of measured coefficients on the fractional error for the bi-exponential case, it can be seen from Fig. 4 that regardless of the values of the measured lifetime components, the error increases (grayscale color becomes darker) as A_1 approaches 0.5. In other words, since $A_2 = 1 - A_1$, the fractional error increases as A_1 and A_2 approach 0.5.

However, the nature of this error trend is not symmetric with respect to A_1. The behavior, as observed in Fig. 4, follows this pattern: if $\tau_2 > \tau_1$ (negative difference), the maximum error tends to occur at values greater than $A_1 = 0.5$ whereas if $\tau_2 < \tau_1$ (positive difference), maximum error tends to occur at values less than $A_1 = 0.5$. Therefore, it is difficult to determine *the specific* A_1 values that would give the maximum error for all cases. However, it is clear that the error from incomplete decay increases for measured coefficients that converge towards 0.5. It is also interesting that although all cases of measured parameters in Fig. 4 followed this error trend with respect to amplitude variations, the magnitude of the error varied drastically between different cases. The reason for this large difference between different cases of measured parameters (lifetime components) will be investigated in the following section.

As shown in Fig. 4, the absolute fractional error between measured (τ_{id}) and original (τ_0) amplitude weighted lifetime values (as defined by Eq. (16) also depends on the measured lifetime components. However, where incomplete decay has an effect, the error does not depend on the magnitude of the measured lifetime components but actually on the differences between the measured lifetime components ($\tau_1 - \tau_2$). It can be observed from Fig. 4 that as the difference between τ_1 and τ_2 increases, the error increases as well. The error trend is not symmetric with respect to the difference between measured lifetime components where positive differences will result in lower error values. This is an indication that larger lifetime component values with the same differences will result in relatively lower fractional error values. Moreover, Fig. 4 demonstrate that in cases with small differences in measured lifetimes (i.e. 4 ns), incomplete decay effects may be negligible (<5%) for all possible coefficient values, which further verifies the threshold values determined by the model.

3.2. The dependency of measured lifetimes (τ_{idn}) on the SNR level

In practical FLIM measurements, the data always includes significant amounts of noise. We performed noise simulation in our model to investigate how noise affects the estimation of amplitude weighted lifetime values. To do this, the simulated noisy incomplete decay curves with the SNR varying from 16 to 182 for various A_{01}:A_{02} ratios (τ_{01} = 1.5 ns (RdmB), and τ_{02} = 4.9 ns (LY)) were fitted using the nonlinear least squares algorithm to obtain the predicted measured amplitude weighted lifetimes (affected by incomplete decay) with noise (τ_{idn}).The corresponding residuals were plotted (data not shown) and at each SNR level showed no pattern, indicating the good quality of fitting process. The original amplitude weighted lifetime values (τ_0) for various A_{01} to A_{02} ratios were also calculated for the original decay signal. Using the inverse model on $\tau_{idn,}$ the corrected amplitude weighted lifetimes were obtained (τ_{corr}). . The original amplitude weighted lifetime (τ_0), predicted measured amplitude weighted lifetimes (with noise) (τ_{idn}), and corrected amplitude weighted lifetimes (τ_{corr}) for various A_{01}:A_{02} ratios at SNR = 16 are shown in Table 4 below. As shown in Table 4, it is demonstrated that the corrected amplitude weighted lifetimes (τ_{corr}) by the inverse model under low SNR = 16 are almost equivalent to the original amplitude weighted lifetimes (τ_0) (less than 1% difference). This further verifies the accuracy of the inverse model and indicates that the effect on estimation error from noise itself is actually minor in comparison with the effect of incomplete decay and is always negligible. This shows that the correction for incomplete decay is indeed necessary.

#146904 - $15.00 USD Received 2 May 2011; revised 21 Jul 2011; accepted 31 Jul 2011; published 2 Aug 2011

Table 4. Simulation values[a]

Original		*Predicted Measured*	*Correction using inverse model on τ_{idn}(ns)*
A_{01} (%)	τ_0 (*ns*)	τ_{idn} (*ns*)	τ_{corr} (*ns*)
0	4.90	4.90	4.90
25	4.05	4.14	4.09
50	3.20	3.29	3.23
75	2.35	2.42	2.37
100	1.50	1.50	1.50

[a]Original amplitude weighted lifetime (τ_0), predicted measured amplitude weighted lifetimes (with noise) (τ_{idn}), and corrected (on τ_{idn}) amplitude weighted lifetimes (τ_{corr}) for various A_{01}:A_{02} ratios at SNR = 16 (τ_{01} = 1.5 ns (RdmB), and τ_{02} = 4.9 ns (LY))

3.3. Experimental results

The fluorescence lifetimes of Lucifer yellow (LY) and Rhodamine B (RdmB) were measured by the time domain TCSPC and the frequency domain ChronosFD systems, which correspond to cases with incomplete decay (in TCSPC, 80 MHz laser is used) and without (in the ChronosFD), respectively. The average lifetime of LY is 5.07 ns ± 0.30 ns (TCSPC) and 4.9 ns ± 0.06 ns (ChronosFD), respectively when fitted with mono-exponential model. RdmB exhibits a fast decay with the fluorescence lifetimes at 1.55 ns ± 0.13 ns and 1.50 ns ± 0.03 ns respectively. In order to determine the original amplitude weighted lifetimes (τ_0) without the effects of incomplete decay, the dye mixture was calculated with respect to the original fluorescence lifetime of each dye obtained from the frequency domain system (4.9 ns and 1.5 ns). Also, to determine the real relative contribution of RdmB and LY (ie correct original coefficients to obtain real original coefficients), the quantum efficiency (QE) of each fluorescence dye was also determined by taking the average of integrated photon intensities from three repetitive LY and RdmB measurements using TCSPC. The results showed the relative QE of RdmB is 36% against LY. Therefore, the quantum efficiency corrected original coefficients can represent the real relative contribution of RdmB ($QE_c\ A_{01}$) and LY ($QE_c\ A_{02}$) where $QE_c\ A_{02} = 1 - QE_c\ A_{01}$.

Table 5 lists the quantum efficiency corrected amplitude weighted lifetimes obtained from frequency domain measurements (τ_0), the TCSPC measurements (τ_{idn}), and correction of τ_{idn} using the inverse model (τ_{corr}). Except for the measurement at $QE_c\ A_{01} =$ 59.1% (τ_0 = 2.89 ns), the measured TCSPC lifetime (τ_{idn}) consistently overestimated the original amplitude weighted lifetime of the solution (τ_0) as obtained from the frequency domain system. The overestimation of measured amplitude weighted lifetime values is predicted and agrees with

Table 5. Experimental values[a]

Frequency domain measurements		*TCSPC with 80 MHz excitation*	*Correction using inverse model on τid_n*	*Differences in τ values*	
$QE_c\ A_{01}$ (%)	τ_0 (*ns*)	τ_{idn} (*ns*)	τ_{corr} (*ns*)	$Diff_{id} = \tau_{idn} - \tau_0$ (*ns*)	$Diff_{corr} = \tau_{corr} - \tau_0$ (*ns*)
0	4.90	5.07	5.07	0.17	0.17
8.2	4.62	4.85	4.76	0.23	0.14
19.4	4.24	4.84	4.34	0.60	0.10
35.2	3.70	3.79	3.76	0.09	0.06
59.1	2.89	2.55	2.49	–0.34	–0.40
100	1.50	1.55	1.55	0.05	0.05

[a]Time domain amplitude weighted lifetimes of Lucifer Yellow (LY) and Rhodamine B (RdmB) mixture solution were measured experimentally using TCSPC (τ_{idn}) and frequency domain lifetime spectrometer (τ_0). Based on the inverse model, the TCSPC measurements were corrected (τ_{corr}) based on an 80 MHz repetition rate excitation. Differences between τ_0 and τ_{idn} ($Diff_{id}$) and between τ_0 and τ_{corr} ($Diff_{corr}$) were evaluated to see whether lifetime estimation error caused by incomplete decay is comparable to errors from random experimental noise.

#146904 - $15.00 USD Received 2 May 2011; revised 21 Jul 2011; accepted 31 Jul 2011; published 2 Aug 2011

the incomplete decay model. Using the inverse model, the measured amplitude weighted lifetime values (τ_{idn}) were corrected and is close enough to the original amplitude weighted lifetime (τ_0) to be within the uncertainties of the experimental measurement. Differences between τ_0 and τ_{idn} ($Diff_{id}$) and between τ_0 and τ_{corr} ($Diff_{corr}$) were evaluated to see whether lifetime estimation error caused by incomplete decay is comparable to errors from random experimental noise. As shown in Table 5, $Diff_{id}$ is always larger than $Diff_{corr}$ for all mixtures indicating that the effect on estimation error from incomplete decay is larger than the effect on error from noise and that the correction for incomplete decay is indeed necessary. The outlier value at 59.1% (τ_0 = 2.89 ns) may be due to low SNR in the experimental measurements, which led to large uncertainties in lifetime estimation for bi-exponential decays.

4. Discussion and Conclusion

Applications of fluorescence lifetime in imaging and spectroscopy have become an active research and technology development area owning to the recent advances of short pulsed lasers and high speed photo detection systems. One of the key technologies that pushing FLIM into a user friendly microscopy modality is the development of turn-key Ti:sapphire laser systems. Although their high repetition rate enables fast image/data acquisition the short interval between consecutive excitation pulses causes concerns that fluorescence lifetime may not be accurately estimated.

In this report, we developed a general mathematical model to quantitatively estimate how incomplete fluorescence decay affects the measured fluorescence decay curves and subsequent estimation of lifetime values. In addition, an inverse model allows the correction of errors caused by incomplete decay. Specifically, the simulation results show that incomplete decay does not affect estimation of individual lifetime component in multi-exponential decays but rather the coefficient terms, which in turn lead to underestimation of average lifetime. As expected, the extent of error strongly depends on the ratio of amplitude weighted lifetime and the interval between excitation pulses. For example, in the case of bi-exponential decay excited at 80 MHz, if both lifetime components are less than 4 ns, the simulation results suggest that the error can be neglected and no correction is required. If at least one lifetime component is larger than 4 ns, the measurement errors would be significant but can be corrected by the proposed mathematical model. Taking individual parameters into account, our results demonstrated that the fractional error between the original and measured lifetime values (E_{id}) became significant with (i) increased laser repetition rate, (ii) converge of coefficients to be equal, and (iii) increased difference between individual lifetime components, while the error is not significantly increased by the noise. These facts offer guidelines that allow researchers to have a better idea for measurement values that may require correction for incomplete decay.

The incomplete decay effect is most profound for fluorophores with long lifetimes such as Photofrin® and ALA induced protoporphyrin IX (PpIX), which are clinically approved photosensitizers with fluorescence lifetimes of more than 10 ns [13]. As a result, invalid interpretation of experimental results can easily happen when the average lifetimes of photosensitizers are measured by short-pulsed lasers with repetition rate more than 20 MHz.

It should be noted that artifacts in lifetime estimation from incomplete decay effect is not significant in microscopy where the lifetimes of most fluorescence probes are short. Nonetheless, in the case of FLIM-FRET, where the majority acceptor-donor pairs have average lifetimes of less than 4 ns while exhibit bi-exponential decay [8], small errors in lifetime estimations may be critical since 5% of lifetime change may corresponding to significant errors in inter-molecular distance calculation.

In addition to applications in microscopy, quantitative analysis of incomplete decay is also useful in other time-domain fluorescence techniques. For example, Yuan *et al.* described a technique that uses fibers with different lengths to multiplex multiple spectral channels of fluorescence decay using a single detector [23]. The multiplexed fluorescence decays were

#146904 - $15.00 USD Received 2 May 2011; revised 21 Jul 2011; accepted 31 Jul 2011; published 2 Aug 2011

separated by the different propagation time introduced by the different fiber lengths. The detected signal is the superposition of signals from decays from adjacent pulses and also suffers from the incomplete decay effect. The inverted model from this work can also correct the superposition of incomplete decays in this case to provide more accurate lifetime estimation.

It should be noted that the reported results were simulated in a scenario with the assumptions that photobleaching is insignificant and the instrumental response function (IRF) is negligibly small. In practice, these assumptions may break down. Therefore, future work includes investigating the models with photobleaching effect and convolution of IRF.

Acknowledgments

The authors acknowledge that this project is supported in part by the Canadian Natural Sciences and Engineering Research Council (NSERC) through the Discovery Grant (Fang) program and Alexander Grant Bell Post Graduate Scholarship (Yeh).

#146904 - $15.00 USD Received 2 May 2011; revised 21 Jul 2011; accepted 31 Jul 2011; published 2 Aug 2011